Collisional and Radiative Processes in a Cesium Afterglow

B. Sayer, J. C. Jeannet, J. Lozingot, and J. Berlande
Service de Physique Atomique, Centre d'Etudes Nucléaires de Saclay, B.P. n°2-91190 Gif-sur-Yvette, France
(Received 6 August 1973)

The evolution of electron density, electron temperature, and population of excited states is measured in a cesium afterglow (pressure range 10^{-3}–2×10^{-2} torr). These are compared with the predictions of a collisional-radiative model. For electron densities between 10^{13} and 10^{11} cm^{-3} and electron temperatures in the range 700–2000 °K, the recombination coefficient is found to be in good agreement with theoretical values. It is proportional to $T_e^{-\gamma}$ with $\gamma = 4.2 \pm 0.4$. The model is shown also to predict accurately the evolution of the electron temperature and excited-state populations. In the late afterglow a change in the ambipolar-diffusion coefficient is observed and is interpreted to be due to a change in the majority ion.

I. INTRODUCTION

In a previous paper,[1] it was shown that the measured steady-state parameters of cesium vapor ionized by means of an electrical discharge are correctly predicted by a so-called collisional-radiative (CR) model, when account is taken of the proper atomic processes. For a given neutral density, the parameters considered are the electron density and temperature, the electric field sustaining the discharge, and the population of excited cesium atoms.

Under transient conditions the model indicates departures from local thermodynamic equilibrium (LTE) generally larger than those predicted for an active discharge and, consequently, the results given by the model are more sensitive to a proper choice of atomic rate coefficients. Thus comparison between experimental and computed data in an afterglow period will be even more fruitful than comparison under steady-state conditions. With only a few exceptions,[2,3] which concern helium, such comparisons in afterglows have been limited to the electron-ion recombination coefficient α, when a collisional-radiative process is supposed to be dominant. For cesium, in spite of much experimental work,[4-8] the kinetic processes of the afterglow are poorly understood and the measured values of α present a large spread. For cesium pressures lower than 10^{-1} torr, α agrees within an order of magnitude with the computed values of the collisional-radiative recombination coefficient. However, owing to a lack of precision in the reported results and the narrow range of experimental conditions, no conclusive comparison with theory was heretofore possible.[9]

It is the purpose of this work to present an extended comparison between the predictions of a collisional-radiative model and experimental results obtained in a cesium afterglow, in the pressure range 10^{-3}–2×10^{-2} torr. In view of the strong dependence of the computed results on the electron concentration n_e and particularly on the electron temperature T_e, very precise measurements of these parameters were achieved. In previous experiments T_e has often only been estimated or measured by probe techniques, which lead to rather large uncertainties. In this work a technique believed to be highly reliable (based on the radiative recombination spectrum) was used and the range of temperatures previously explored was extended down to temperatures as low as 700°K. A microwave heating system enables us to vary selectively T_e and thus to obtain a precise determination of the dependence of the atomic processes on this parameter.

In Sec. II of this article we present briefly the most important features of the collisional-radiative model that has been used. In Sec. III we describe the experimental apparatus and the diagnostic techniques. Section IV is devoted to experimental results and a comparison with theory.

II. COLLISIONAL–RADIATIVE MODEL

The model used in this work has been presented in previous articles.[1,10] We consider an ionized cesium vapor composed of Cs^+ ions, electrons, and excited cesium atoms (48 levels are considered). The continuity equations for each excited state (density n_p) and for free electrons (density n_e) are written

$$\frac{dn_p}{dt} = n_e\left[n_e K_p^{\text{rec.}} + \sum_{q\neq p} n_q K_{q,p}^{\text{exc.}}\right] + \sum_{q>p} n_q A_{q,p} + n_e^2 \beta_p - n_p\left[n_e\left(K_p^{\text{ion}} + \sum_{q\neq p} K_{p,q}^{\text{exc.}}\right) + \sum_{q<p} A_{p,q}\right], \quad (1)$$

$$\frac{dn_e}{dt} = n_e \sum_p n_p K_p^{\text{ion}} - n_e^2 \left[\sum_p K_p^{\text{rec.}} + \beta_p \right], \qquad (2)$$

where K are the rate coefficients for inelastic collisions with electrons: K_p^{ion}, ionization from level p; $K_{p,q}^{\text{exc.}}$, excitation from p to q; $K_p^{\text{rec.}}$, recombination on level p by three-body collision ($K_p^{\text{rec.}} \sim n_e$). A are the spontaneous-emission coefficients and β the radiative recombination coefficients. To take into account the reabsorption of resonance lines, we have multiplied the corresponding A coefficients by a transparency factor, which is, for our experimental conditions, equal to 10^{-3}.

The energy balance of the free electrons is written

$$\frac{dW_e}{dt} = \frac{d(\frac{3}{2} n_e k T_e)}{dt} = \left(\frac{dW_e}{dt}\right)_{\text{el. col.}} + \left(\frac{dW_e}{dt}\right)_{\text{in. col.}} + \left(\frac{dW_e}{dt}\right)_{\text{rad.}} + \left(\frac{dW_e}{dt}\right)_{\text{dif.}}, \qquad (3)$$

where the terms on the right-hand side represent, respectively, the contributions of elastic collisions with atoms and ions,[11] the inelastic collisions with atoms, and losses due to radiative recombination and diffusion. Writing

$$\frac{dn_e}{dt} = \left(\frac{dn_e}{dt}\right)_{\text{rec.}} + \left(\frac{dn_e}{dt}\right)_{\text{dif.}}$$

and assuming that the electrons lost by diffusion have the mean energy $\frac{3}{2} kT_e$, Eq. (3) can be written

$$\tfrac{3}{2} kT_e \left(\frac{dn_e}{dt}\right)_{\text{rec.}} + \tfrac{3}{2} k n_e \frac{dT_e}{dt} = \left(\frac{dW_e}{dt}\right)_{\text{el. col.}} + \left(\frac{dW_e}{dt}\right)_{\text{in. col.}} + \left(\frac{dW_e}{dt}\right)_{\text{rad.}}. \qquad (3')$$

It should be noted that, under the assumption made for the energy of the electrons lost by diffusion, the energy-balance equation (3′) does not contain any diffusion term.

The system of equations (1), (2), and (3′) can be used to compute the values of n_e, T_e, and n_p in a steady-state regime, as was done in Ref. 1. In such a case each of the equations of the system is set equal to zero. For the case of a decaying plasma it is possible, making some approximations, to avoid solving a system of differential equations. (a) If T_e and n_p remain in quasiequilibrium with n_e, that is to say, if Eqs. (1) and (3) are set equal to zero, Eq. (2) gives dn_e/dt, from which the recombination coefficient is calculated[10]:

$$\alpha = -\frac{1}{n_e^2} \left(\frac{dn_e}{dt}\right)_{\text{rec.}}.$$

(b) On the other hand, if we consider n_e and T_e as independent parameters, the first derivatives of n_e and T_e are deduced from Eqs. (2) and (3′), Eq. (1) being set equal to zero.

These two approximations are referred to as cases II and III in Table I.[12] We shall see later that they may be used to predict the evolution of various parameters for two different regimes of the afterglow. The validity of such approximations is related to the respective values of the relaxation frequencies of n_e, T_e, and n_p, as discussed by McWhirter and Hearn.[13]

TABLE I. Comparison of the three solutions of the model.

	Independent parameters	Set of equations to be solved	Computed parameters
Steady state	n_1, n_e (or T_e),	$\frac{dn_p}{dt} = 0$	T_e (or n_e)
I		$\frac{dT_e}{dt} = 0$	n_p
	T_g	$\frac{dn_g}{dt} = 0$	Power input
Quasi-steady-state	n_1, n_e, T_g	$\frac{dn_p}{dt} = 0$	T_e
(T_e and n_p)		$\frac{dT_e}{dt} = 0$	n_p
II			$\frac{dn_e}{dt}$
Quasi-steady-state	n_1, n_e, T_e, T_g	$\frac{dn_p}{dt} = 0$	n_p
(n_p only)			$\frac{dn_e}{dt}$
III			$\frac{dT_e}{dt}$

III. APPARATUS AND DIAGNOSTIC TECHNIQUES

The experimental setup and the diagnostic techniques have previously been described in det. il.[1] The cell (Fig. 1) is a cylindrical glass tube (6 cm diameter) which has been outgased (10^{-8} torr residual pressure) and sealed after introducing cesium. It is placed in an oven and the cesium pressure is controlled by regulating the tempera-

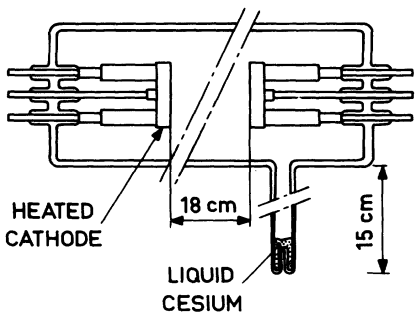

FIG. 1. Experimental cell (scale $\frac{1}{4}$).

ture of an oil bath surrounding an appendix which contains liquid cesium. A current pulse of about 2.5-msec duration is applied between two electrodes, a heated cathode (900°C) and a cold anode, made of two coaxial molybdenum disks separated by 18 cm.

The electron density is measured using a free-space microwave interferometer ($\lambda = 4$ mm). A sensitivity of a few thousandths of a degree phase shift is achieved, corresponding to an electron density of about 10^8 cm^{-3}.

The electron temperature T_e is deduced from the spectrum of radiative recombination on the $6P$ level. This method, which has been described by Agnew,[14] consists of plotting $\log[\lambda^2 I(\lambda)]$ vs $1/\lambda$, where λ is the wavelength and I the intensity of radiation; the curve obtained is a straight line with a slope proportional to T_e^{-1}. This method gives results more reliable than those given by probe techniques. It is less sensitive to departure from LTE than the other optical methods, which are based on measurement of line intensities. The precision is estimated to be a few tens of degrees.

The populations of various excited states are deduced from absolute-line-intensity measurements. The absolute intensities are obtained by comparing the emitted light with that of a standard source. The appropriate Einstein coefficients[15] are taken from theoretical data of Stone[16] and Warner,[17] and from the experimental values of Agnew and Summers,[14] and Gridneva and Kasabov.[18]

The measurements of electron density, electron temperature, and population of excited states are made in a plane equidistant from cathode and anode, along a diameter; consequently, the Abel inversion method is used on the recombination spectrum and line intensities[1] to deduce the values of n_e, T_e, and n_p on the axis of the tube.

An amplitude-controlled microwave generator is used to heat selectively the electrons.[19] The source is an X-band klystron working either in the dc or pulse regime (5 W maximum power). A wave guide which terminates in an open-ended metallic cylinder surrounding the discharge tube connects the source to the ionized vapor. The distribution in the plasma of the microwave electric field cannot be calculated in such a configuration. When heating is applied, T_e is therefore measured and found uniform around the region of observation. As shown in Fig. 2, the rise time of the electron temperature is short in comparison to the characteristic decay time of the afterglow. The temperature T_e may be deduced, as indicated previously, from the measurement of the continuum. However, this method becomes rather imprecise at low electron density because the emitted light is weak. Under these circumstances the increase of the

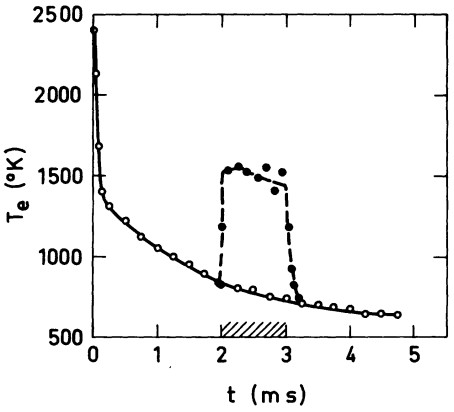

FIG. 2. Decay of electron temperature during the afterglow and influence of a microwave heating pulse ($P_{Cs} = 2.10^{-2}$ torr).

electron temperature from T_e to T_{eH} is deduced from the lowering of the intensity I of the light emitted by very high excited levels (14 F, for example) according to

$$I_H/I = (T_e/T_{eH})^{3/2}\, e^{(E_i/k)(1/T_{eH} - 1/T_e)},$$

where E_i is the ionization energy of the upper state of the transition. This method is obviously limited to the determination of those fast variations of the electron temperature where the change of electron density is negligible.

IV. EXPERIMENTAL RESULTS

Before comparing the predictions of the CR model with the experimental data in the early afterglow, we will first consider the diffusion processes in the late afterglow.

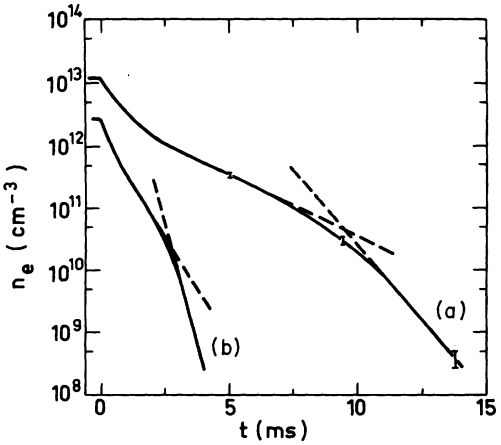

FIG. 3. Decay of electron density during the afterglow for pressures of 10^{-2} torr (a) and 2.5×10^{-3} torr (b).

A. Diffusion Processes in the Late Afterglow

In the pressure range we have investigated ($10^{-3} \leq P_{Cs} \leq 2\times10^{-2}$ torr) the electron-density-decay curves (Fig. 3) are characterized in the late afterglow ($n_e < 10^{12}$ cm^{-3}) by two exponential parts separated by a transition region. Independent of the pressure, the transition region corresponds to an electron density between 10^{11} and 10^{10} cm^{-3}. The time constants τ_1 and τ_2 of the two exponential decays are approximately in the ratio 2:1.

An exponential decay of the electron density during the afterglow is generally characteristic of a regime controlled by ambipolar diffusion (for the electron densities considered here). If this interpretation seems valid for the very late afterglow ($n_e < 10^{10}$ cm^{-3}) where $\log n_e$ varies linearly with time over almost two orders of magnitude of n_e, it may be contested for the first part of the late afterglow ($10^{10} < n_e < 10^{12}$ cm^{-3}). For a further check we have measured the change of the electron-decay time constant τ when a microwave pulse heats the electrons. In a regime governed by ambipolar diffusion, τ is related to the electron temperature according to

$$\frac{1}{\tau} = \frac{D_a}{\Lambda^2} = \frac{D_i}{\Lambda^2}\left(1 + \frac{T_e}{T_i}\right),$$

where D_a and D_i are the ambipolar and the ion diffusion coefficients, Λ the diffusion length, and T_i the ion temperature. Thus τ changes to τ_H when, as a result of heating, T_e increases to T_{eH}:

$$\frac{\tau}{\tau_H} = \frac{T_i + T_{eH}}{T_i + T_e}.$$

On the assumption that T_i was equal to the oven temperature, it was checked experimentally that this relation is verified when $n_e < 10^{12}$ cm^{-3} [in the transition region τ is defined as $n_e(dn_e/dt)^{-1}$]. It is concluded that the whole late afterglow is controlled by ambipolar diffusion. We shall see in Sec. IV B that the "time constant" τ of the early afterglow is affected quite differently by a heating pulse.

In Fig. 4, the ratios P_{Cs}/τ ($\tau = \tau_1$ and τ_2) are plotted as a function of cesium pressure. These ratios are observed to be independent of the pressure and equal, respectively, to 5 and 11 torr sec^{-1} ($D_{a\,1,2} P_{Cs}$ are equal to, respectively, 14 and 33 torr cm^2 sec^{-1}). These results indicate that, in the pressure range investigated, no diffusion cooling is present, supporting the assumption made in Eq. (3′); i.e., the electrons lost by diffusion have a mean energy which does not differ significantly from $\frac{3}{2}kT_e$.

From the constant ratios P_{Cs}/τ_1 and P_{Cs}/τ_2 we deduce the reduced mobilities μ_{10} and μ_{20} of the ions present in the afterglow:

$$\mu_{10,20} = (2.1\times10^3)\frac{P_{Cs}}{\tau_{1,2}}\frac{\Lambda^2}{T_g^2}\ \text{cm}^2\,\text{V}^{-1}\,\text{sec}^{-1},$$

where the diffusion length is equal to 1.74 cm and the gas temperature T_g is assumed to be equal to the oven temperature (610°K). We obtain $\mu_{10} = 0.08$ cm^2 V^{-1} sec^{-1} and $\mu_{20} = 0.18$ cm^2 V^{-1} sec^{-1}.

The first value may be compared with those measured by Dandurand and Holt[5] (0.066) in an afterglow, by Chanin and Steen[20] (0.075), Lee and Mahan[21](0.12), and Popescu and Niculescu[22](0.14) in a drift tube, and with the theoretical estimation by Sheldon[23] (0.036–0.088) for the mobility of the Cs^+ ion in its parent vapor. The second value may be compared with the mobilities measured by Chanin and Steen,[20] Lee and Mahan[21] (0.2), and Popescu and Niculescu[22] (0.30), which are generally attributed to Cs_2^+ ions in the absence of mass-spectroscopic identification. In spite of the large spread of those results we tentatively conclude that Cs^+ is the majority ion when $n > 10^{11}$ cm^{-3}, while Cs_2^+ ions are predominant when $n_e < 10^{10}$ cm^{-3}, for the pressure range we have investigated. We have not found a simple mechanism able to interpret this change in the identity of the majority ion. Our observations are to be compared to those of Morgulis and Korchevoi,[24] who have measured, with a mass spectrometer, an increase of the Cs_2^+/Cs^+ ratio when the electron density in an active discharge is lowered.

In the rest of this paper our interest is only concerned with the electron density range where recombination effects are significant with respect to diffusion losses ($n_e > 10^{11}$ cm^{-3}).

B. Collisional–Radiative Processes in the Early Afterglow

We now compare the measured values of some parameters of the early afterglow with those de-

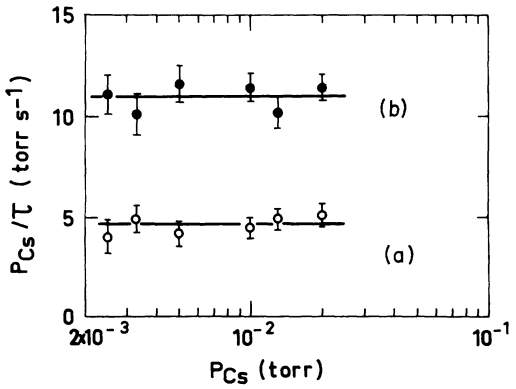

FIG. 4. P_{Cs}/τ vs pressure for the first exponential decay of electron density (a) and for the second (b).

duced from the CR model. This comparison is first carried out on the electron-ion recombination coefficient, then extended to the evolution of elecron temperature and population of excited states. This would therefore provide a relatively complete test of the model.

1. *Recombination Coefficient*

The evolution of electron density in an afterglow may be described by the following equation, assuming only one ionic species is present:

$$\frac{\partial n_e}{\partial t} = -\alpha(n_e, T_e) n_e n_i + D_a(T_e)\nabla^2 n_e, \qquad (4)$$

where α is the recombination coefficient and S an electron source term. We shall neglect the source term because reactions involving electrons, such as

$$Cs^* + e \rightarrow Cs^+ + 2e,$$

are taken into account in the collisional-radiative recombination mechanism; those involving neutral particles, such as

$$Cs^* + Cs \rightarrow Cs_2^+ + e \text{ or } Cs^* + Cs^* \rightarrow Cs_2^+ + e,$$

may be neglected because of the low density of the excited atoms in the appropriate states during the afterglow and the cross sections of these processes.[25] Because of electric neutrality Eq. (4) becomes

$$\frac{\partial n_e}{\partial t} = -\alpha n_e^2 + D_a \nabla^2 n_e. \qquad (4')$$

It is possible to compare the measured electron density decay with a numerical solution of Eq. (4'), where α is expressed as a analytical function of n_e and T_e.[26] A more simple and direct way, which will be used here, is to assume that the electron spatial distribution is never far from the Bessel function J_0 and, therefore, write Eq. (4') as

$$\frac{dn_e}{dt} = -\alpha n_e^2 - \frac{n_e}{\tau_D}. \qquad (4'')$$

τ_D is a characteristic time constant for ambipolar diffusion which is a function of T_e (i.e., a function of time during the afterglow):

$$\tau_D = \tfrac{1}{2}\tau_1(1 + T_e/T_i), \qquad (5)$$

where τ_1 is the time constant of the first exponential decay (see above). Using equations (4'') and (5) we have deduced the values of α from the electron-density-decay curves. The results obtained by this simplified method have been compared with those deduced from the analytical solution of the partial derivative equation (4'), in which α has been expressed as $\alpha = A n_e T_e^{-4.5}$: an agreement better than the experimental uncertainties has been observed.

The three-body recombination coefficient $K(K = \alpha/n_e)$ has been plotted as a function of T_e for two pressures (Fig. 5). It is seen that K is independent of pressure and proportional to $T_e^{-4.2\pm0.4}$. This temperature dependence is in good agreement with the theoretical predictions concerning collisional-radiative recombination[9,10,27-30] ($T_e^{-4.5}$ in the electron-density and temperature range of our experiment). The absolute value of K agrees also with the theoretical ones: they are about 50% lower than the results of Sayer and Pascale[10] and a factor 2 lower than the values of Mansbach and Keck.[30]

The recombination coefficients found in this work are slightly lower than those deduced by Wada and Knechtli[31] from electron-density balance in a steady-state thermal plasma. Good agreement is observed with the recombination coefficient measured by Hammer and Aubrey[32] using a Cs^+ beam. It is interesting to compare our results with those obtained by Aleskovskii[6] using, as we did, an afterglow technique. The large discrepancy observed (a factor of 5 to 10) may be explained by an inaccuracy in his electron-temperature measurement. Aleskovskii used both radiative-recombination-spectrum and probe techniques. The recombination continuum has been interpreted using the data of Mohler and Boeckner[33]; the resulting temperatures have to be lowered in view of the

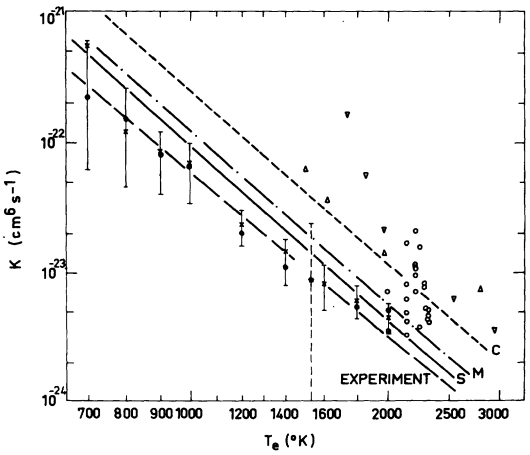

FIG. 5. Three-body recombination coefficient K vs electron temperature. Theoretical data by Curry, Ref. 9 (C); Mansbach and Keck, Ref. 30 (M); Sayer and Pascale, Ref. 10 (S). Experimental results by Wada and Knechtli, Ref. 31 (○); Hammer and Aubrey, Ref. 32 (*); Aleskovskii, Ref. 6, for $P_{Cs} = 1.5\times10^{-2}$ torr (△) and $P_{Cs} = 5\times10^{-3}$ torr (▽); and present results for $P_{Cs} = 2\times10^{-2}$ torr (×) and 10^{-2} torr (●).

more recent results of Agnew.[14] Measurements by a probe technique are known often to overestimate the electron temperature.[34-36] An overestimation of about 500°K, as observed in a stationary discharge,[1] could explain the discrepancies between our data and those of Aleskovskii.

A confirmation of our results was obtained by varying T_e using controlled microwave heating of the electrons. This increase of T_e induces a change in the experimental value of τ, which then becomes τ_H. The ratio τ_H/τ can also be predicted from Eqs. (4″) and (5), since

$$\frac{1}{n_e}\frac{dn_e}{dt} = \frac{1}{\tau} = -K(T_e)n_e^2 - \frac{2T_i}{\tau_1(T_e+T_i)} .$$

τ_H/τ has been calculated (Fig. 6) for $K=(2.4\times10^{-10})T_e^{-4.2}$, as deduced from our experimental results (curve e); for $K=(3\times10^{-9})T_e^{-4.5}$, as given by the theoretical model of Sayer and Pascale[10] (curve m), and for K values multiplied (curve m$^-$) and divided (curve m$^+$) by a factor of 2; for the cases of the regime of pure diffusion ($K=0$) and that of pure collisional-radiative recombination ($\tau_1=\infty$) (curves d and r).

Except for $n_e>2\times10^{12}$ cm^{-3}, where the heating is probably inhomogeneous because n_e greatly exceeds the cutoff density for the microwave frequency used, the measured ratios τ_H/τ are, within error bars, in good agreement with those calculated using the experimental K values (curve e).

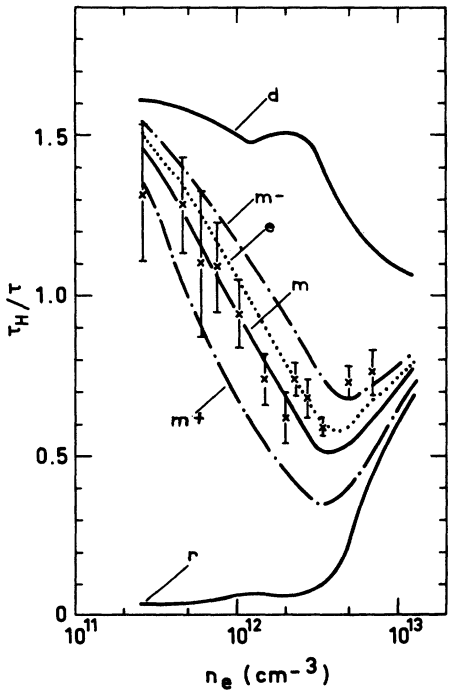

FIG. 6. Ratios of the slopes of the curves $\log n_e = f(t)$ with and without heating ($P_{Cs}=2\times10^{-2}$ torr). Measured ratios (×) are compared to those calculated (see text).

2. *Relation between Electron Temperature and Electron Density*

On Fig. 7 we compare the variation of T_e as a function of electron density during the afterglow with that predict by the model. On this figure, curves a and b represent the relations $T_e=f(n_e)$ computed, respectively, for steady-state and quasi-steady-state conditions referred to in Table I as cases I and II.

Point A corresponds to the experimental conditions before turning off the discharge current. The position of this point, close to curve a, confirms the validity of the model to represent the steady-state conditions.[1] This indicates also that the pulse duration (2.5 msec) is sufficiently long, for our pressure conditions (0.02 torr), to reach the steady-state regime.

The other experimental points corresponds to the afterglow period. From point B down to the lowest electron densities there is excellent agreement between experimental results and the computed curve b, which shows that the quasistationary approximation gives a very good representation of the decay of the electron temperature.

Between points A and B the electron temperature changes rapidly without any significant variation of the electron density. During this short period (about 100 μsec) of the very early afterglow, T_e is not in quasiequilibrium with the electron density (case III of Table I).

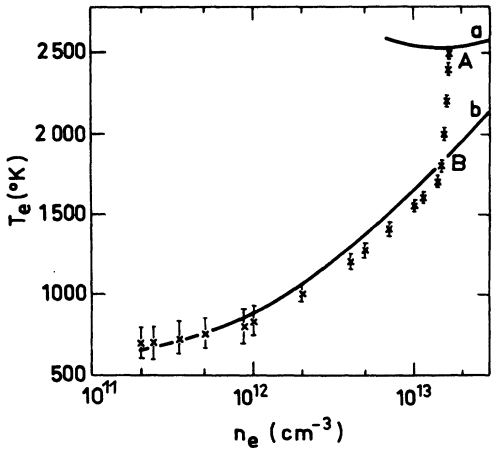

FIG. 7. Relation between electron temperature and density during the afterglow. Curve a has been computed for the steady-state conditions and curve b for the quasi-steady-state conditions. The crosses correspond to the experimental data.

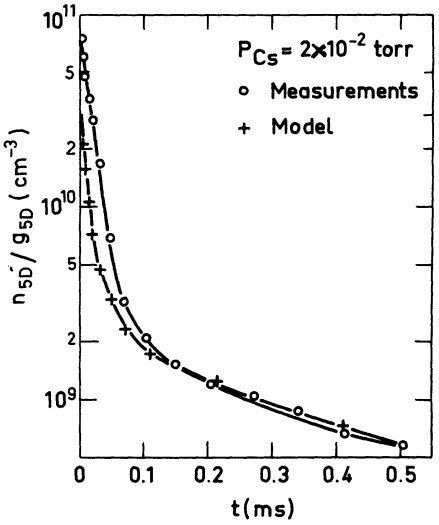

FIG. 8. Decay of the population of the $5D$ level, deduced from the intensity of the $6S$-$5D$ transition (spontaneous emission coefficient given by Sayer *et al.* Ref. 37).

3. *Population of Excited States*

For comparison of theory and experiment we have chosen to consider the evolution of the population of atoms in certain excited states during the first part of the afterglow, and the departure from LTE of the excited F levels in the later afterglow.

The early afterglow includes the period corresponding to the fast decay of the electron temperature (from A to B on Fig. 7). In this case approximation III of Table I, that is, n_e and T_e considered as independent parameters, has been used to calculate the decay of the excited-state populations. Experimentally three types of decay curves have been observed, as illustrated by Figs. 8, 9, and 10, which correspond to levels $5D$, $11F$, and $8S$, respectively.

The population of level $5D$, which may be considered as a "low" level (ionization energy $E_i = 2.1$ eV, excitation energy 1.8 eV), decreases very rapidly, in agreement with theory (Fig. 8). During the discharge this level is mainly populated by direct excitation from the ground state or by a two-step process involving the $6P$ state. Therefore the excitation efficiency, which depends strongly on electron temperature, decreases rapidly at the very beginning of the afterglow.

Level $11F$ is closely coupled with free electrons ($E_i = 0.1$ eV). Thus, the population of this level is close to that given by the Saha–Boltzmann equation (i.e., proportional to $n_e^2 T_e^{-3/2} e^{E_i/kT_e}$). During the very beginning of the afterglow the fast decay of T_e leads to an increase of the population. The population reaches a maximum at $t \simeq 100$ μsec in the afterglow, which roughly corresponds to point B of Fig. 7, and then decreases under the predominant influence of electron-density decay.

Level $8S$ ($E_i = 0.9$ eV) is an "intermediate" level, the population of which is proportional to $\rho\, n_e^2 T_e^{-3/2} e^{E_i/kT_e}$, where ρ characterizes the departure from LTE. This factor, which is larger than 1 during the discharge, becomes very rapidly lower than 1 during the early afterglow (first tens of microseconds). Its variation is then slowed down and the influence of T_e and n_e on the population becomes successively preponderant, as in the case of $11F$ level. Therefore the decay curve presents both a relative minimum and a relative maximum (Fig. 10).

It is seen on Fig. 11 that the highest F levels ($n > 12$) are in LTE with the electron gas, as was assumed in the model.[38] The lower F levels are

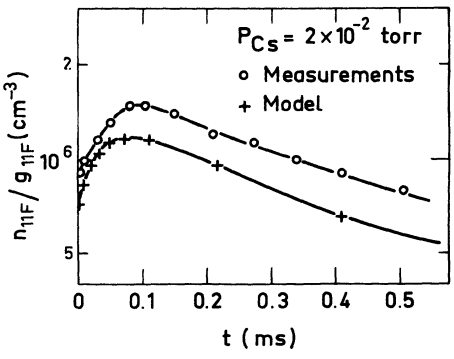

FIG. 9. Decay of the population of the $11F$ level, deduced from the intensity of the $5D$-$11F$ transition (A value of Agnew and Summers, Ref. 14).

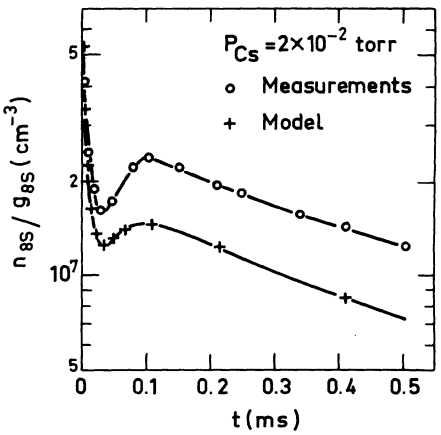

FIG. 10. Decay of the population of the $8S$ level, deduced from the intensity of the $6P$-$8S$ transition (A value of Stone Ref. 16).

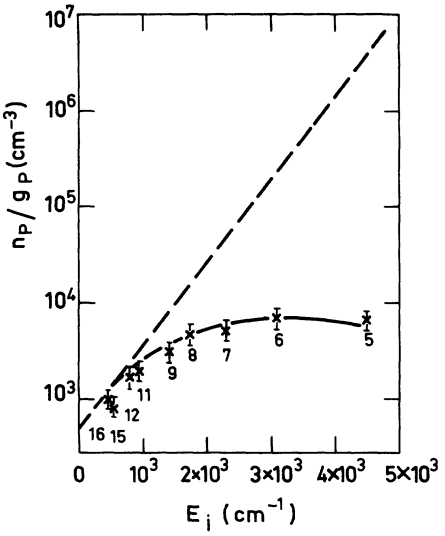

FIG. 11. Population of nF levels ($5 \leq n \leq 16$) as a function of ionization energy. $P_{Cs} = 2\times10^{-2}$ torr, $n_e = 2\times10^{11}$ cm^{-3}, and $T_e = 700°K$. LTE conditions, dashed line; model, solid line; experiment, crosses. We have used A_{5D-nF} values of Stone (Ref. 16) extrapolated for the highest terms of the series.

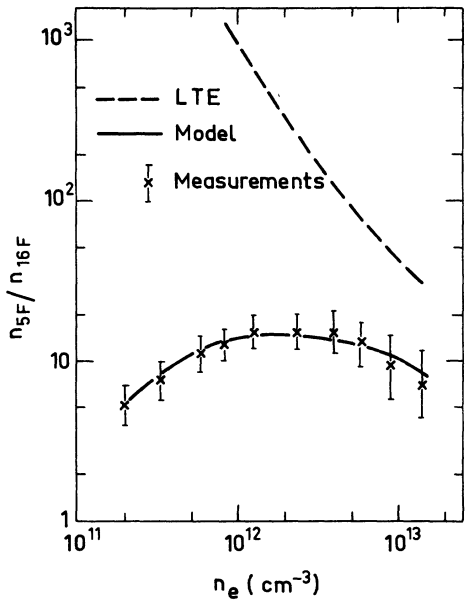

FIG. 12. Ratio of the population of the $5F$ and the $16F$ levels ($P_{Cs} = 2\times10^{-2}$ torr).

underpopulated with respect to the LTE predictions; their populations fit well to the values computed with the model, even at low electron densities, for which the departure from LTE reaches several orders of magnitude. This departure increases when the electron density decreases, as shown in Fig. 12, where the population ratio of levels $5F$ and $16F$ is plotted.

V. CONCLUSION

The study of the early cesium afterglow ($10^{11} < n_e < 10^{13}$ cm^{-3}) in the pressure range 10^{-3} to 2×10^{-2} torr, using precise optical diagnostics, has indicated that a collisional-radiative model is able to predict with very good accuracy not only the electron–Cs^+-ion recombination coefficient, but also the relation between electron density and electron temperature during their decay, and the evolution of excited-state populations. The residual differences between experimental data and computed results (which appear in Figs. 8–10) are, in our opinion, of the order of the precision which can be obtained with such a model. For this reason, we did not try to improve the quality of the agreement by varying some of the atomic parameters (inelastic electron-atom cross sections) used in the model, as was done by Johnson and Hinnov[3] for helium. The agreement is sufficiently good to enable one to deduce, for example, electron density and temperature from line intensity measurements, even when the populations of the various excited states deviate from LTE by several orders of magnitude.

Measurements of the three-body recombination coefficient K yielded a dependence of K upon T_e of the form T_e^{γ}, where $\gamma = -4.2 \pm 0.4$, confirming theoretical prediction in a relatively wide range of electron temperature, 700–2000°K.

ACKNOWLEDGMENTS

The authors are grateful to Professor L. Goldstein, Professor D. E. Kerr, and Dr. W. E. Wells for their criticism of the manuscript. They acknowledge the stimulating interest of Dr. C. Manus.

[1]B. Sayer, J. C. Jeannet, and J. Berlande, J. Phys. (Paris) 33, 993 (1972).
[2]F. Robben, W. B. Kunkel, and L. Talbot, Phys. Rev. 132, 2363 (1963).
[3]L. C. Johnson and E. Hinnov, Phys. Rev. 187, 143 (1969).
[4]F. L. Mohler, J. Res. Natl. Bur. Stand. (U.S.) 19, 447 (1937).
[5]P. Dandurand and R. B. Holt, Phys. Rev. 82, 278 (1951).
[6]Yu. M. Aleskovskii, Zh. Eksp. Teor. Fiz. 44, 840 (1963) [Sov. Phys.—JETP 17, 570 (1963)].
[7]D. Balfour and J. H. Harris, in *Proceedings of the*

Seventh International Conference on Phenomena in Ionized Gases (Gradevinska Knjiga, Beograd, 1965), Vol. 1, p. 32.
[8]S. Von Goeler, R. W. Mottley, and R. Ellis, Phys. Rev. 172, 162 (1968).
[9]B. P. Curry, Phys. Rev. A 1, 166 (1970).
[10]B. Sayer and J. Pascale, C. R. Acad. Sci. (Paris) 273, 453 (1971).
[11]W. L. Nighan, Phys. Fluids 10, 1085 (1967).
[12]In Table I, T_g is the heavy particle temperature (atoms and ions), which appears in the elastic collision term of the energy balance of free electrons [Eq. (3)].
[13]R. W. P. McWhirter and A. G. Hearn, Proc. Phys. Soc. Lond. 82, 641 (1963).
[14]L. Agnew and C. Summers, in Ref. 7, Vol. 2, p. 574.
[15]We have used in the model the A values deduced from the calculations of Anderson and Zilitis (Ref. 39) because they are the only complete set of data for all the radiative transitions considered by the model (some thousands). These values are probably less precise than that the computed excited-state populations are not very sensitive to small changes in the A coefficients.
[16]P. M. Stone, Phys. Rev. 127, 1151 (1962); Phys. Rev. 135, AB2E (1966).
[17]B. Warner Mon. Not. R. Astron. Soc. 139, 115 (1968).
[18]J. M. Gridneva and G. A. Kasabov, in Ref. 7, Vol. 2, p. 581.
[19]L. Goldstein, J. M. Anderson, and G. L. Clark, Phys. Rev. 90, 151 (1953).
[20]L. M. Chanin and R. D. Steen, Phys. Rev. 132, 2554 (1963).
[21]Y. Lee and B. H. Mahan, J. Chem. Phys. 43, 2016 (1965).
[22]A. Popescu and N. D. Niculescu, in *Proceedings of the Ninth International Conference on Phenomena in Ionized Gases* (Institute of Physics, Bucarest, 1969).
[23]J. W. Sheldon, J. Appl. Phys. 34, 444 (1963).
[24]N. D. Morgulis and Yu. P. Korchevoi, Zh. Eksp. Teor. Fiz. Pis'ma Red. 9, 313 (1968) [JETP Lett. 8, 192 (1968)].
[25]R. S. Bergman and L. M. Chanin, in *Proceedings of the Tenth International Conference on Phenomena in Ionized Gases* (Donald Parsons, Oxford, England, 1971).
[26]B. Sayer and J. Berlande, Phys. Lett. 21, 636 (1966).
[27]D. R. Bates, A. E. Kingston, and R. W. P. McWhirter, Proc. R. Soc. Lond. A267, 297 (1962).
[28]J. V. Dugan, Jr., NASA Report No. TND-2004.
[29]D. W. Norcross and P. M. Stone, J. Quant. Spectrosc. Radiat. Transfer 8, 665 (1968).
[30]P. Mansbach and J. Keck, Phys. Rev. 181, 275 (1969).
[31]J. Y. Wada and R. C. Knechtli, Phys. Rev. Lett. 10, 513 (1963).
[32]J. M. Hammer and B. B. Aubrey, Phys. Rev. 141, 146 (1966).
[33]F. L. Mohler and C. Boeckner, J. Res. Natl. Bur. Stand. (U.S.) 2, 489 (1929).
[34]G. Wehner and G. Medicus, J. Appl. Phys. 23, 1035 (1952).
[35]H. M. Musal, J. Appl. Phys. 41, 2605 (1970).
[36]J. M. Buzzi, H. J. Doucet, and D. Gresillon, Phys. Fluids 13, 3041 (1970).
[37]B. Sayer, R. Wang, J. C. Jeannet, and M. Sassi, J. Phys. B. 4, L20 (1971).
[38]An estimate of the photoionization rate of these excited levels, in the presence of the radiation of the hot cathode, indicates that it is several orders of magnitude smaller than the electron ionization (or excitation) rate.
[39]E. M. Anderson and V. A. Zilitis, Opt. Spectrosc. 16, 211 (1964).